The hydrodynamics of air-filled bags for wave energy conversion

Greaves, Deborah; Hann, Martyn; Kurniawan, Adi; Chaplin, John; Farley, Francis

Publication date:
2016

Document Version
Publisher's PDF, also known as Version of record

THE HYDRODYNAMICS OF AIR-FILLED BAGS FOR WAVE ENERGY CONVERSION

D. Greaves & **M. Hann**, *Plymouth University, UK*
A. Kurniawan, *Aalborg University, Denmark*
J. R. Chaplin & **F. J. M Farley**, *University of Southampton, UK*

ABSTRACT

The search for an economic means to harness energy from ocean waves continues. This paper aims to summarise the findings from our recent studies of novel wave energy devices in which flexible, deformable structures are used in place of conventional rigid structures. The devices utilise a flexible air-filled bag to capture energy from the waves and three different configurations are compared. In each of the three device configurations, expansion and contraction of the bag in waves create a reciprocating air flow via a turbine between the bag and another volume. The bags are all in the form of a fabric encased within an array of longitudinal tendons. In the first configuration, the bag is floating and ballasted such that it pierces the free surface. In the second configuration, the bag is completely submerged and connected at its top to a rigid float and at its bottom to a weight. In the third configuration, the bag is fixed at its bottom and free at the top. A series of tests at approximately 1:20 scale in the laboratory was conducted to investigate the static behaviour of the bags in still water and their dynamic response in waves. Numerical models are developed for each configuration and the predictions agree closely with measurements. Both reveal some interesting properties that are distinct from one device configuration to another.

1. INTRODUCTION

Over 40 years have passed since Stephen Salter discussed the idea of large-scale utilisation of energy from ocean waves [1]. Many different wave energy devices have been proposed, incorporating a wide range of modes of operation, but as yet they show no signs of converging into one single solution.

In recent work funded by the UK EPSRC, we have investigated the potential to reduce the cost of wave energy through the use of deformable fabric structures for wave energy conversion. Deformable bodies can have several advantages over their conventional rigid counterparts. In particular, a heaving deformable body can have a longer resonance period than that of a heaving rigid body of the same size, because of the lower hydrostatic stiffness [2]. This means that the device can be smaller and hence cheaper if a deformable body is used. Further advantages of fabric structures are that they are lightweight, they do not require as much material as rigid structures for the same given volume, and they have excellent fatigue properties.

Motivated by this idea, Farley [3, 4] proposed a compressible wave energy device in the form of a heaving wedge that opens and closes as it heaves in waves (see Fig. 1). This action pumps air, enclosed by the wedge, into and out of a secondary volume via a turbine. The resonance period of the device depends on the stiffness of the wedge, which is governed by the internal air volume.

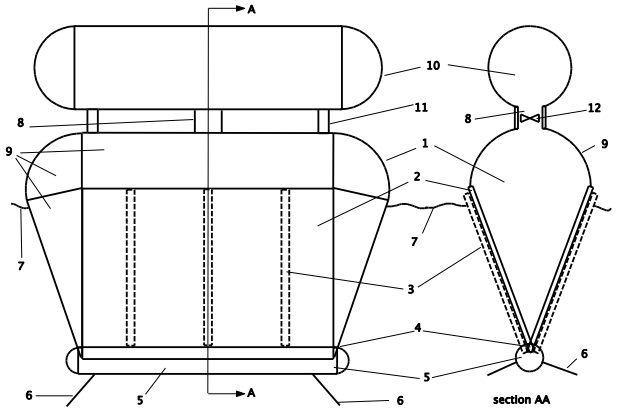

Fig. 1 The free floating clam device, reproduced from [3, 4]

A series of studies has then been devoted to similar devices employing the same power take-off (PTO) principle, but with a completely flexible bag as the deformable body (see Fig. 2). The first of these (A) is a floating device, where the ballasted bag pierces the free surface. The second (B) is also a floating device, but with a completely submerged bag connected at its top to a rigid float [5]. In the third device (C), the bag is fixed at its bottom and free at the top. All three devices are axisymmetric. V1 denotes the volume enclosed by

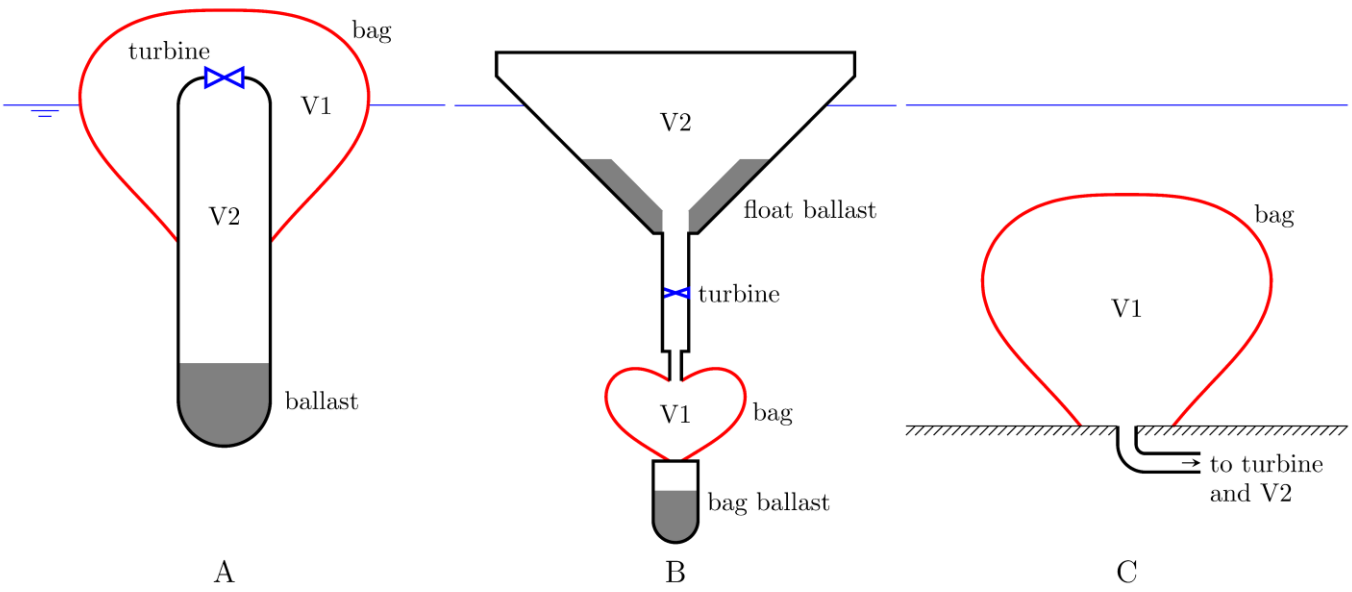

Fig. 2 Schematics of the three axisymmetric devices, adapted from [14, 15]. Device C can be submerged or surface piercing

the bag, while V2 denotes the secondary volume. A turbine separates V1 from V2. As will be shown in this paper, these differences in configuration result in distinct behaviour among the three devices.

The bags in the devices are all in the form of a fabric encased within an array of longitudinal tendons (see Fig. 3). When the bag is inflated, the fabric forms lobes between the tendons. This effectively keeps the tension in the fabric to a minimum, and the tendons become the major load-bearing members. Such bags have been used mainly for aerospace applications [6], but recently also underwater [7, 8]. In air, where the difference between internal and external pressure is approximately uniform, the bag takes a pumpkin-like shape [9]. Immersed in water, the shape is more like that of an inverted pear due to increasing external hydrostatic pressure with depth.

Each of the three devices has been studied by a combination of physical experiments and numerical modelling [10-15]. This paper summarises the results of these studies and compares the three devices in terms of their static and dynamic behaviour, and their wave absorbing performance.

2. EXPERIMENTAL SETUP

Physical tests of the devices at approximately 1:20 scale were carried out in the ocean wave basin, measuring 35m × 15.5m, with a water depth of 3m, at Plymouth University's COAST Laboratory.

In order for the resonance frequency to be scaled correctly, the volumes of V1 and V2 had to be considerably larger than those implied by the cube of the scale factor, since the compressibility of air is the same in the model as in the prototype. Without these additional volumes, the air stiffness and resonance frequency of the device would be unrealistically high. Accordingly, V1 was augmented by the volume of an additional air chamber (or a series of chambers), which was connected to the top of the bag by a flexible hose, and to a similar chamber (or a series of chambers) representing V2, as seen in Fig. 3. The chambers were mounted on the gantry spanning the wave basin.

The duct between V1 and V2 housed a PTO in the form of an assembly of parallel capillary pipes in which the air flow was laminar, providing a linear PTO of predictable damping [16].

The bags had 16 tendons, and the fabrics were made of unreinforced polyurethane film. For devices A and B, ballast was provided by lead shot inside a cylindrical steel container with a hemispherical base, mounted beneath the bag.

The pressures in V1 and V2 were recorded by pressure transducers. A manometer was used to monitor the pressure in the system at all times.

The heave motion of the device was recorded using a string potentiometer or infrared cameras. In addition, two video cameras, above and under water, recorded the device motions from the side.

Fig. 3 Photographs of the test setup and model of device A in the wave basin

3. NUMERICAL MODEL

3.1 STATIC SHAPE

To calculate the equilibrium shape of the bag in still water, we assume that all forces are transferred to the tendons. Since the bag is axisymmetric and the lobes are neglected, the shape of the bag is determined by the profile of a single tendon, running from the top to the bottom of the bag.

The tendon is first discretised into a number of arc elements with unknown radii of curvature. The radius of each element is obtained by solving the force equilibrium in the direction normal to the element. In static conditions, the forces acting on the element are the internal air pressure, the tendon tension, and the external hydrostatic pressure if the element is submerged.

The calculation starts from the top of bag and proceeds piecewise downward along the tendon. The top elevation of the bag and the tendon tension are not known beforehand, so an iterative process is required to obtain the correct tension and top elevation to give the specified radius at the bottom of the bag. The problem resembles the two-dimensional problem of inflatable dams under static loading, and the solution procedure is similar [17, 18]. We add further simplifying assumptions that the tendons are both massless and inextensible.

For devices A and B, the equilibrium position of the device in the water, as well as the tangent of the tendon at the top of the bag for device B, are found by requiring that the sum of vertical forces on any part of the device and on the device as a whole must be zero.

3.2 DYNAMIC MODEL

To predict the device response in waves, each device is modelled using the classical linear frequency-domain approach. This essentially means that time-harmonic motions of small amplitudes about the mean or static position are assumed. The approach consists of first establishing the static equations for the device, including for each element of the discretised bag. Then the static equations are expanded by expressing any time-dependent quantity as the sum of its static component and its dynamic component. Subtracting the static equations from the expanded equations and keeping only terms up to the first order yield a set of linear equations of motion for the device. Since time-harmonic motions are assumed, the resulting equations of motion can be expressed in terms of complex amplitudes. For simplicity, only heave and axisymmetric motions of the bag are considered.

The dynamic forces acting on each tendon element include the dynamic air pressure inside the bag, the dynamic tendon tension, and the dynamic water pressure outside the bag. The dynamic air pressure inside the bag is related to the volume change of the bag, and is assumed to follow isentropic relations for an ideal gas. In addition, the flow through the turbine is assumed to be proportional to the pressure difference between V1 and V2. The dynamic water pressure outside the bag is the sum of the excitation pressure due to the waves incident on the device and the waves scattered by the device; the radiation pressure due to the motions of the device including the bag, conventionally decomposed into an added mass and a radiation damping terms; and lastly a hydrostatic restoring component due to the change of buoyancy arising from the displacements of the device. A panel method [19] may be used to compute the excitation and radiation pressures.

Once the equations of motion are solved, the mean absorbed power in waves can be obtained, as further described, e.g. in [14].

4. RESULTS AND DISCUSSION

The numerical model has been extensively validated, showing good agreement with experimental measurements, both in the static and dynamic cases. The reader is referred to [10-12, 14, 15] for further details.

4.1 STATIC BEHAVIOUR

Due to the deformable nature of the bag, varying the amount of air in the device changes its equilibrium geometry. For devices A and B, this also changes their draught (see Fig. 4). For device C, the internal pressure decreases as expected as the bag is deflated. For devices A and B, the

behaviour is subtler. For device A, as the bag is deflated from near full inflation, the internal pressure first decreases and then increases. For device B, the pressure first decreases and then increases, before decreasing again. Plotting the elevation of any point on the device against the device internal pressure results in a C-shaped curve for device A and an S-shaped curve for device B.

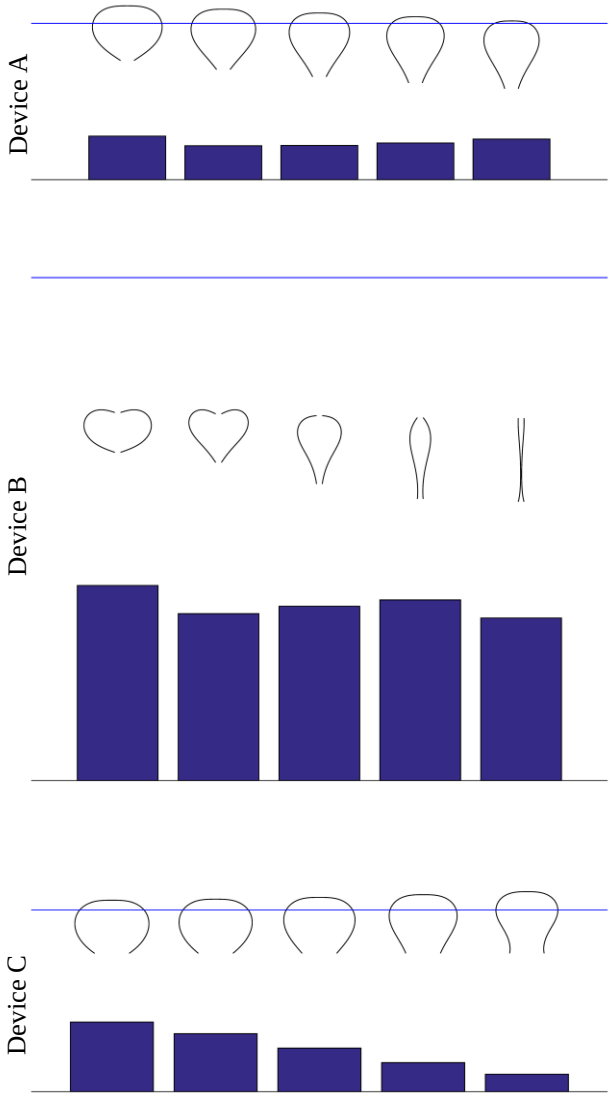

Fig. 4 Variation of the bag shape (top) and the corresponding bag pressure (bottom) with decreasing amount of air in the bag, for devices A, B, C. The blue horizontal lines indicate the mean water surface

These behaviours of devices A and B may be explained as follows. Near full inflation, the bag is tight, and releasing air from the bag decreases the pressure without changing its volume much. Further deflation reduces the bag's volume further and causes the device to go down to provide the required buoyancy, and this increases the internal pressure because of the increasing external hydrostatic pressure. Device A would finally sink after some point when there is not enough buoyancy to balance the weight of the device. For device B, however, since the rigid float provides excess buoyancy, the device does not sink even after all air is released, hence the S-shaped trajectory of device B in contrast to the C-shaped trajectory of device A.

The S- and C-shaped curves mean that depending on the amount of air in the bag, device A can have two different equilibrium bag shapes for the same bag pressure, while device B can have three different equilibrium bag shapes for the same bag pressure.

4.2 COMPARISON OF PERFORMANCE BETWEEN DEVICE CONFIGURATIONS

The performance of the devices is compared in terms of the capture width ratio, which is defined as the ratio of the device capture width to the water plane diameter. The typical capture width ratio for each device is plotted in Fig. 5 against the normalised wave length, defined as the ratio of the wave length to the water plane diameter. The PTO damping is not optimised at every frequency, but set to a specific value for all frequencies. The capture width ratios of devices A and B are also compared with those of rigid devices of the same geometries as devices A and B, absorbing through heave against a fixed reference. The PTO damping is set equal to the radiation damping at the heave resonance period of the rigid device.

Compared to their rigid counterparts, devices A and B have longer resonance period, demonstrating that potential cost saving can be achieved through the use of deformable bodies. The bandwidth is narrower, but only slightly.

Comparing devices A and B, we see that device B has a broader bandwidth. However, the maximum capture width ratio of device B is less than that of device A, implying that to capture the energy from the same wave length, a larger water plane area than that of device A is required for device B.

To have a peak absorbed power at a target wave period of 8 seconds, device A would need to have

a water plane diameter of 14.5 m. The bag would have a volume of 1400 m^3, while the required volumes of V1 and V2 corresponding to the result shown in Fig. 5 would be 700 m^3 and 450 m^3, respectively. The displacement of the device would be about 1400 tonnes.

Device B, on the other hand, would need a water plane diameter of 20 m to have a peak absorbed power at 8 seconds. The volume of the bag is 85 m^3, as the bag for device B is smaller than that of device A. The device displacement would be 1200 tonnes. The volumes of V1 and V2 corresponding to the result shown in Fig. 5 would be about 1200 m^3 each. These volumes, which are larger than the submerged volume of the device, would have to be contained above the float, or be external to the device.

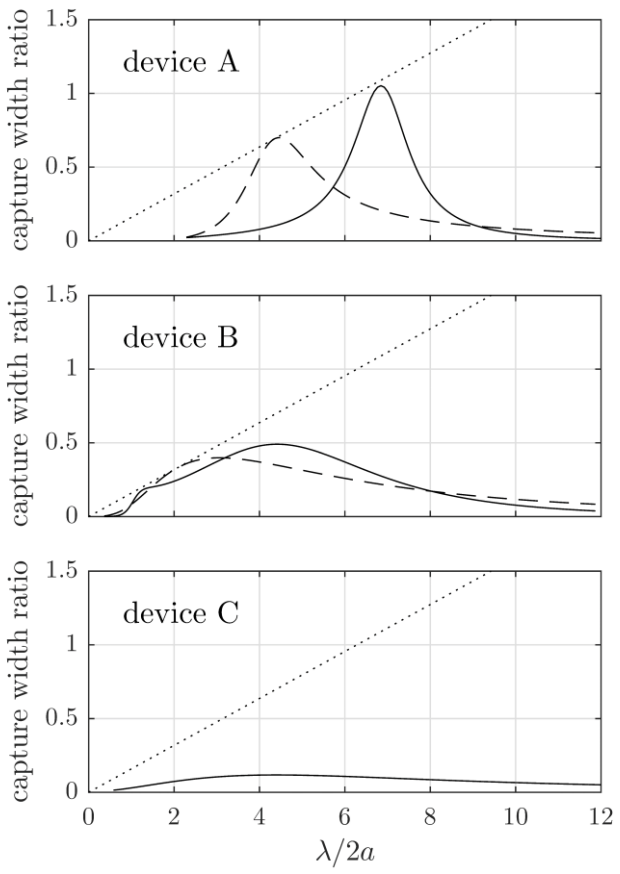

Fig. 5 Typical capture width ratios of devices A, B, and C as function of normalised wave length. For devices A and B, dashed lines are the capture width ratios of heaving rigid devices of the same geometries as devices A and B. Dotted lines are the maximum theoretical limit for point absorbers

Among the three devices, device C does not capture much power relative to the incident wave power. The reason seems to be the relatively little volume change compared to that of device A or B. Note that it is possible for the bag to change its shape without much change in its volume.

To have a peak absorbed power at 8 seconds, the water plane diameter of device C would need to be about 12 m. The bag would have a volume of 750 m^3, and the volumes of V1 and V2 would be 700 m^3 and 2400 m^3, respectively. V2 would be external to the device. The mean buoyancy of the bag would be 500 tonnes.

4.3 ADVANTAGES & DISADVANTAGES

As discussed above and shown in Fig. 5, the deformable nature of the bag brings about an advantage to floating heaving devices A and B in lengthening their resonance period compared to that of rigid devices of a similar size. This is achieved without the need of active control. Furthermore, devices A and B do not require any external reference. The expansion and contraction of the sealed bag pump air into and out of the secondary volume, the pressure change in which acts at the same time to generate a restoring force on the bag. The same of course applies to device C, but whereas some ballast is required to balance the buoyancy of devices A and B, some downward force is required to balance the buoyancy of the bag for device C.

A motivation for device B was to introduce a double-peaked response to the system. The first peak, at a longer wave period, would correspond to the float and the bag ballast moving in phase, while at the second peak, at a lower wave period, the float and the bag ballast would be moving in anti-phase. The second peak is evident for example from Fig. 5 at a wave length of about the water plane diameter. This interaction may be responsible for a broader absorption bandwidth in device B compared to that of device A.

Nevertheless, the relative displacement between the float and the bag ballast for device B cannot be greater than the length of the bag's tendons. This implies that there is a limit to the maximum power that can be absorbed by the device.

Due to the buoyancy provided by the float, device B does not sink with bag deflation or failure, unlike device A.

In terms of their potential locations of installation, device C, since it is fixed at the bottom, would be limited to nearshore sites, while devices A and B, since they are floating, could be installed further offshore. Also device C would be susceptible to the effect of tidal variations of water depth on the hydrodynamic characteristics of the bag, although this could possibly be compensated by changes to the internal pressure. A possible advantage associated with being close to shore is that the power take-off and some of the air volume for device C can be located on shore.

5. CONCLUSIONS

A significant drawback of wave energy converters acting as heaving point absorbers is that they have to be large in order to operate optimally in swell waves. To overcome these limitations, control systems may be used in order to modify the motion response to suit the wave climate, but this can be complex and expensive.

We have investigated an alternative approach in which the device's geometry responds to hydrodynamic loading. Each of the axisymmetric devices considered in this paper comprises a sealed bag that expands and contracts without hinges. This breathing action makes it possible to install a power take-off inside the device that requires no external reference. The breathing action can be used to exchange air through a turbine with a second volume. No other mechanical parts are needed because the pressure change in the second volume generates a restoring force on the bag.

The potential benefits of deformable fabric structures in a wave energy device have been demonstrated. The floating devices considered in this study both can have resonance periods longer than that of a rigid heaving device of a similar size, which means that devices employing flexible structures can be made smaller than the more conventional rigid devices. Furthermore, the flexible fabric bag is lightweight and may be deflated for storage and transport. These are expected to result in significant cost saving. Also, owing to its compliant nature, the bag is naturally capable of taking concentrated loads, which will be important for ensuring its survivability in storm conditions.

Studies on the various load cases, material selection, manufacturing methods, in addition to optimisation and control strategies will be essential to progress to the next level.

ACKNOWLEDGEMENTS

This work is supported by the Engineering and Physical Sciences Research Council through the SuperGen Marine Energy Research Consortium [EP/K012177/1]. Malcolm Cox of Griffon Hoverwork Ltd supplied the model-scale bags and offered practical insights.

REFERENCES

1. Salter, S. H., 1974 ‘Wave power’, Nature Vol. 249, pp. 720-724
2. Kurniawan, A., Greaves, D., and Chaplin, J., 2014 ‘Wave energy devices with compressible volumes’, Proc. R. Soc. A 470: 20140559
3. Farley, F. J. M., 2011 ‘The free floating clam – a new wave energy converter’, Proc. 9th European Wave and Tidal Energy Conf., Southampton, UK, 5-9 September 2011
4. Farley, F. J. M., 2012 ‘Free floating bellows wave energy converter’, Patent GB2488185, filing date: 9 May 2011, publication date: 22 August 2012
5. Farley, F. J. M., 2016 ‘Wave power converter’, Patent application GB2532074, filing date: 9 November 2014, publication date: 11 May 2016
6. Pagitz, M., 2007 ‘The future of scientific ballooning’, Phil. Trans. R. Soc. A Vol. 365 No. 1861, pp. 3003-3017
7. Pimm, A. J., Garvey, S. D., and de Jong, M., 2014 ‘Design and testing of energy bags for underwater compressed air energy storage’, Energy Vol. 66, pp. 496-508
8. de Jong, M., 2014 ‘Commercial grid scaling of Energy Bags for underwater compressed air energy storage’, International Journal of Environmental Studies
9. Taylor, G. I., 1963 ‘On the shapes of parachutes’, in The Scientific Papers of G. I. Taylor (ed. G. K. Batchelor), pp. 26-37,

Cambridge University Press (Original work published 1919)
10. Chaplin, J., Farley, F., Kurniawan, A., Greaves, D., and Hann, M., 2015 'Forced heaving motion of a floating air-filled bag', Proc. 30th Int. Workshop on Water Waves and Floating Bodies, Bristol, UK
11. Chaplin, J., Farley, F., Greaves, D., Hann, M., Kurniawan, A., and Cox, M., 2015 'Numerical and experimental investigation of wave energy devices with inflated bags', Proc. 11th European Wave and Tidal Energy Conference, Nantes
12. Kurniawan, A., Greaves, D., Hann, M., Chaplin, J., and Farley, F., 2016 'Wave energy absorption by a floating air-filled bag', Proc. 31st Int. Workshop on Water Waves and Floating Bodies, Plymouth, US
13. Kurniawan, A. and Greaves, D., 2016 'Wave power absorption by a submerged balloon fixed to the sea bed', IET Renewable Power Generation
14. Kurniawan, A., Chaplin, J. R., Greaves, D. M., Hann, M., and Farley, F. J. M., 'Wave energy absorption by a floating air bag' (arXiv:1608.04874)
15. Chaplin, J. R., Kurniawan, A., Hann, M. Greaves, D., and Farley, F. J. M., 'Wave energy absorption by a submerged air bag connected to a rigid float' (in preparation)
16. Chaplin, J. R., Heller, V., Farley, F. J. M., Hearn, G. E., and Rainey, R. C. T., 2012 'Laboratory testing the Anaconda', Phil. Trans. R. Soc. A 370, pp. 403-424
17. Harrison, H. B., 1970 'The analysis and behaviour of inflatable membrane dams under static loading', Proc. Inst. Civil Eng. 45, pp. 661-676
18. Parberry, R. D., 1976 'A continuous method of analysis for the inflatable dam', Proc. Inst. Civil Eng. 61, pp. 725-736
19. WAMIT, 2013, WAMIT, Inc., Chestnut Hill, MA. Version 7.0